Adsorption Mechanism of Lead on Wood/Nano-Manganese Oxide Composite

Al Abdullah, Jamal*+

Department of Protection and Safety, Atomic Energy Commission, Damascus, P.O. Box 6091, SYRIAN ARAB REPUBLIC

Al Lafi, Abdul Ghaffar

Department of Chemistry, Atomic Energy Commission, Damascus, P.O. Box 6091, SYRIAN ARAB REPUBLIC

Alnama, Tasneem; Al Masri, Wafa'a; Amin, Yusr

Department of Protection and Safety, Atomic Energy Commission, Damascus, P.O. Box 6091, SYRIAN ARAB REPUBLIC

Alkfri, Mohammed Nidal

Department of Physics, Atomic Energy Commission, Damascus, P.O. Box 6091, SYRIAN ARAB REPUBLIC

ABSTRACT: *Discharge of untreated industrial wastewater containing heavy metals such as Pb^{2+} is hazardous to the environment due to their high toxicity. This study reports on the adsorption, desorption, and kinetic study on Pb^{2+} removal from aqueous solutions using wood/Nano-manganese oxide composite (WB-NMO). The optimum pH, contact time and temperature for adsorption were found to be 5.0, 4 h and 333 K, respectively. Pseudo-second-order kinetics best described the adsorption process with an initial sorption rate of 4.0 mg g min^{-1}, and a half-adsorption time $t_{1/2}$ of 31.6 min. Best fit for adsorption isotherm was obtained with the Brunauer-Emmett-Teller (BET) model with a maximum adsorption capacity of 213 mg/g for an initial metal concentration of 60 mg/L. Both intra-particle diffusion and film diffusion contribute to the rate-determining step. Desorption experiments with 0.5 mol/L HCl, inferred the reusability of the composite. Adsorption experiment of Pb^{2+} from industrial wastewater confirmed that the prepared WB-NMO is a promising candidate for wastewater treatment. The WB-NMO demonstrated high Pb^{2+} removal efficiency and is considered as a promising alternative and reusable composite for lead removal from contaminated effluents.*

KEYWORDS: *Wood; Manganese oxide; adsorption; Kinetics; Lead.*

* *To whom correspondence should be addressed.*

+ E-mail: prscientific@aec.org.sy

1021-9986/2018/4/131-144 14/$/6.04

INTRODUCTION

Water contamination with heavy metals, such as lead (Pb), receives considerable attention from scientists and engineers due to their toxic nature. Even at low concentrations, lead may cause a range of health effects including behavioral problems, and learning disabilities (*WHO* 2008; *Cechinel et al.* 2014). Therefore, the World Health Organization (WHO) [1] recommended a maximum acceptable concentration of lead in drinking water of less than 0.01 mg/L (*WHO* 2008). Several sources of lead pollution can threat the natural water sources in the surrounding area, i.e. urban or industrial activities; such as batteries, dyes, glass and paint coatings (*WHO* 2008; *Özcan et al.* 2009; *Eren et al.* 2009; *Al Abdullah et al.* 2014; *Li et al.* 2010).

Numerous technologies have been investigated for metal ions removal from wastewater. Sorption as a convenient method has been widely used to immobilize ions onto a solid phase surface (*Eren et al.* 2009; *Šćiban et al.* 2007; *Maliyekal et al.* 2010; *Eberhardt and Min* 2008; *Shi et al.* 2015; *Sanchooli Moghaddam et al.* 2016; *Yousefpour* 2017; *Tajiki and Abdouss* 2017).

Although different materials from natural or man-made origin have been investigated as promising adsorbents, the focus of researchers has recently been directed towards the use of natural materials, such as agricultural by-products, olive stones, nut shells, coffee and tea waste, spent grain, rice husks, leaves, wood bark and sawdust from various trees (*Cechinel et al.* 2014; *Mohan et al.* 2014; *Miró et al.* 2008; *Kalavathy et al.* 2005; *Wu et al.* 2005; *Božić et al.* 2013; *Hegazi* 2013; *Zhu, Zongqiang et al.* 2013; *Pehlivan* and *Kahraman* 2011; *Yargıç et al.* 2015; *Martín-Lara et al.* 2014). The high availability and low cost of such materials make them more beneficial than the conventional adsorbents or ion exchange resins.

In addition, the use of many types of woods including wood sawdust, mango, maple, poplar, pine, almond shell, and oak has been investigated as a promising sorbent for the adsorption of hazardous metal ions from wastewater, but with limited efforts for significantly improving the properties of the used biosorbents (*Božić et al.* 2013; *Hegazi* 2013; *Pehlivan* and *Kahraman* 2011; *Semerjian* 2010; *McLaughlan et al.* 2015; *Ishaq et al.* 2016).

Recently, it has been shown that various Nanostructured Manganese Oxides (NMO) can be prepared through a simple, low cost and eco-friendly route by the reduction of $KMnO_4$ by inorganic acids or alcohols (Chen and He 2008; *Al Lafi* and *Al Abdullah* 2015; *Al Abdullah et al.* 2016; *Al Lafi et al.* 2016). However, NMO has not been widely applied in environmental remediation due to several engineering limitations such as the difficulty in solid–liquid separation, leaching of NMO along with the treated effluent and the low hydraulic conductivity. Moreover, the presence of other ions with NMO in aqueous solution can cause aggregation of nanoparticles, and thereby reduce its reactivity. This phenomenon of ion induced aggregation of nanoparticles in aqueous suspension may be prevented by anchoring the nanoparticles on suitable matrices (*Maliyekkal et al.* 2010; *Al Lafi* and *Al Abdullah* 2015; *Al Abdullah et al.* 2016; *Al Lafi et al.* 2016).

Wood is considered an appropriate material due to its hierarchically porous structure, with a micrometer the scale of transverse ray parenchyma and fiber, and a nanometer scale of molecular fiber and cell membrane (*Greil* 2001).

In this work, wood biosorbent-NMO composites (WB-NMO) have been prepared and their structural, morphological and adsorption properties were investigated. The experimental data obtained by batch assay have been analyzed using kinetics and adsorption isotherms. Moreover, the reusability of WB-NMO has been discussed to obtain a treatment process with lower production of residues. The results of this study were applied to industrial wastewater and the efficiency for the adsorption of lead as an alternative to conventional processes was evaluated.

EXPERIMENTAL SECTION

Materials

Poplar wood waste, one of the most wood wastes produced in the country, was collected from a local company in Damascus. Real wastewater samples were collected from a local factory of battery production in Damascus. The main characteristics of these samples are: pH=2.95, Pb = 20.0±0.2 mg/L, So_4^{2-} = 240±5 mg/L and Ca^{2+} = 60±2 mg/L. All reagents used were of analytical grade, and working concentrations of Pb^{2+} ion were obtained by diluting a standard solution of $Pb(NO_3)_2$ (1000 mg/L) to desired values.

Adsorbent preparation and characterization

All wood samples were air-dried, crushed, sieved with different meshes (100-2000 μm), and the mean size (500-800 μm) was taken in the present study. The biosorbent (WB) was prepared by treating wood samples with 4 % w/w NaOH solution for 24 h, washing several times with super pure water, and finally drying in an oven at 353 K.

The composite; WB-NMO was prepared by impregnating WB in $KMnO_4$ solution (0.03 mol/L), and heating at 333K for 12 h in a drying oven. When the liquid content reached 10 %, the reaction mixture was dried at 355 K for further 2 h. WB-NMO samples were washed several times with super pure water to get rid of un-reacted chemicals, and finally dried at 363 K to a constant weight and stored in polyethylene bottles for further use.

Stability tests of WB-NMO with respect to pH effect were carried out by equilibrating 0.1 g of composite samples in 150 ml of super pure water at different pH values in the range 2-12, and keeping them in an automatic shaker at 295±2 K for 24 h. Solutions were then filtered and the total manganese content was determined.

The point of zero charge (pH_{PZC}) was determined by acid-base titration according to the procedure outlined by M. Davranche et al. (2003).

The manganese loading in WB-NMO samples was determined by acid digestion method. For this, 0.2 g of WB-NMO samples were leached with 100 mL HCl solution (6 mol L^{-1}). Results showed that the manganese oxide contents in the composite samples were in the range 2-10 %.

Instruments

The concentrations of Mn and Pb ions were measured using Atomic Absorption Spectroscopy (AAS-Perkin-Elmer 2380 instrument). The quality of the analysis was checked with internal certified samples, and procedural blanks were run with samples in a similar way for quality assurance of the laboratory analysis. The accuracy of the analysis was ±5 % for all elements. The Pb^{2+} standard solution from Fisher Scientific® was analyzed in the same manner for analysis accuracy check. Results showed that the errors in the analysis were less than 5 %.

A STADI-P STOE Transmission Diffractometer, with CuK_α radiation (λ= 1.54060 Å) and a germanium monochromatic operated at 50 kV and 30mA was used to record the X-Ray powder Diffraction (XRD) patterns in a range of 5-90° (2θ). Fourier Transformation InfraRed (FT-IR) spectra were recorded using a Nicolet 6700 FT-IR spectrometer operating on the ATR mode. All spectra were measured from 400 to 4000 at a resolution of 4cm^{-1} and a total of 64 scans. A separate background spectrum was subtracted in each collection. Scanning Electron Microscopy (SEM) images were taken by a Tescan Vega II XMU scanning electron microscope operated at 20 kV.

Adsorption experiments

Batch adsorption experiments were carried out in 250 mL falcons, with a lead solution volume of 200 mL. After the addition of WB-NMO, the falcons were immediately shaken at 200 rpm in an automated shaker at 295±2 K.

The effect of agitation time was studied for periods ranging from 15 min to 6 h, at v/m= 0.07 g/L and lead concentration of 5.0 mg/L. The pH of the solution was kept constant at 5.0±0.2. Effects of adsorbent dose were investigated at a pH of 5.0±0.2 and Pb^{2+} concentration of 10, 25 and 60 mg/L. The pH effect on Pb^{2+} adsorption was also investigated by varying the pH from 2.5-10 using diluted solution of NaOH (0.01 mol/L), with lead concentration of 1.3 mg/L at 295±2 K. The effect of pH was studied at low concentration of Pb^{2+} to avoid the precipitation of $Pb(OH)_2$ at high pH value.

The percentage removal of Pb^{2+} was calculated using Eq. (1):

$$\%\ \text{Removal} = 100 \times (c_o - c_e)/c_o \quad (1)$$

Where c_o and c_e are the initial and equilibrium concentrations of Pb^{2+}, respectively.

The data obtained in batch studies were used to calculate the equilibrium metal uptake capacity using the following equation:

$$q_e = (c_o - c_e) \times v/m \quad (2)$$

Where v (L) is the solution volume and m (g) is the adsorbent mass.

Column adsorption study

Column adsorption experiments were conducted with real wastewater produced from the battery industry. As one important and growing sector where the use of non-toxic and non-hazardous substitute materials has not rapidly developed in such industry.

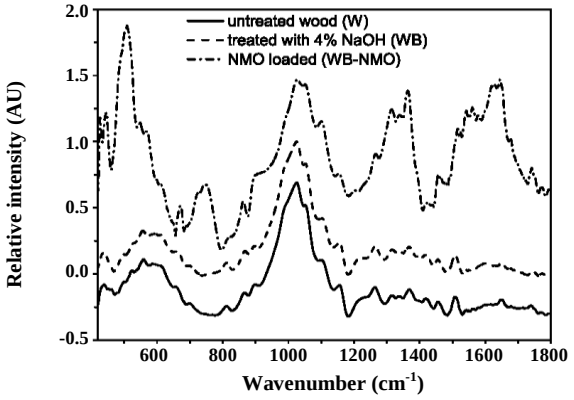

Fig. 1: The FT-IR spectra of wood before and after alkali treatment and the FT-IR spectrum of the composite material.

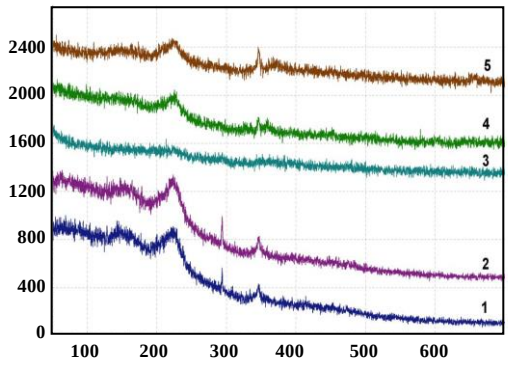

Fig. 2: X-ray powder diffractograms of wood samples: (1) untreated wood (W); (2) wood biosorbent (WB) and (3-5) WB-NMO with different NMO loading (3 being the highest), respectively.

Real Pb^{2+} wastewater at pH 5.0±0.2 was fed through the column (10 cm in length packed with 10.0 g of WB-NMO, the equivalent to a packing height of 6.5 cm, with an internal diameter of 2.5 cm) by a peristaltic pump with a flow rate of 4 mL/min and operation time of 24 h. The temperature was maintained at 295±2 K. Effluent samples were collected at several time intervals and analyzed for lead.

RESULTS AND DISCUSSION

Characterization of W, WB and WB-NMO

It is well known that wood mainly consists of cellulose, hemi-cellulose, and lignin (*Wiedenhoeft* and *Miller* 2005). The NaOH solution was used to clean and modify wood surfaces according to the following reaction:

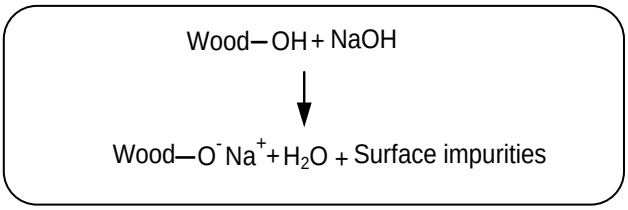

Fig. 1 shows that the intensity of several IR absorption bands was slightly reduced after alkali treatment. These include the bands at 1737, 1515 and 1254 cm^{-1}, which are assigned to a CO stretching vibration of ester in hemicellulose, the benzene ring vibration of lignin and to a CO stretching vibration of the acetyl group in lignin component (*Morán et al.* 2008; *Sreenivasan et al.* 1996). The results indicated a partial removal of hemicellulose and the cross links which is lignin, and as a result the porosity of the lignocellulosic materials is increased (*Sun* and *Cheng* 2002). The major effect of alkaline pretreatments is the delignification of lignocellulosic biomass, thus enhancing the reactivity of the remaining carbohydrates.

X-ray results for wood samples before and after treatment are shown in Fig. 2. Alkali treatment has been reported to reduce the proportion of crystalline material present in wood, as observed by several researchers (*Sreenivasan et al.* 1996; *Gassan* and *Bledzki* 1999). However, as shown in Fig. 2, alkali treatment did not change the structure of wood, which may be attributed to the improvement of the order of crystallites after alkali treatment (*Gassan* and *Bledzki* 1999).

After the treatment with $KMnO_4$, the previous bands at 1737, 1515 and 1254 cm^{-1} were disappeared indicating that these bands were involved in the oxidation reaction of wood. This is consistent with that the treatment with $KMnO_4$ selectively oxidizes lignin moieties to create carboxylic and ester functions (Jolly et al. 2006).

As shown in Fig. 2, the XRD pattern of the wood were reduced due to the deposition of NMO on the surface of wood, and disappeared in the sample corresponding to the highest NMO loading. Moreover, no crystalline patterns were observed for NMO, which may be attributed to the amorphous oxide phase or the formed nano structure of the oxide.

The SEM micrographs of wood samples are presented in Fig. 3. The SEM of untreated wood in Fig. 3 (a) shows the radial surface of tracheids, and bordered pits are clearly visible. The warty membrane that lines the lumen is also clearly visible, especially in Fig. 3 (b) where it

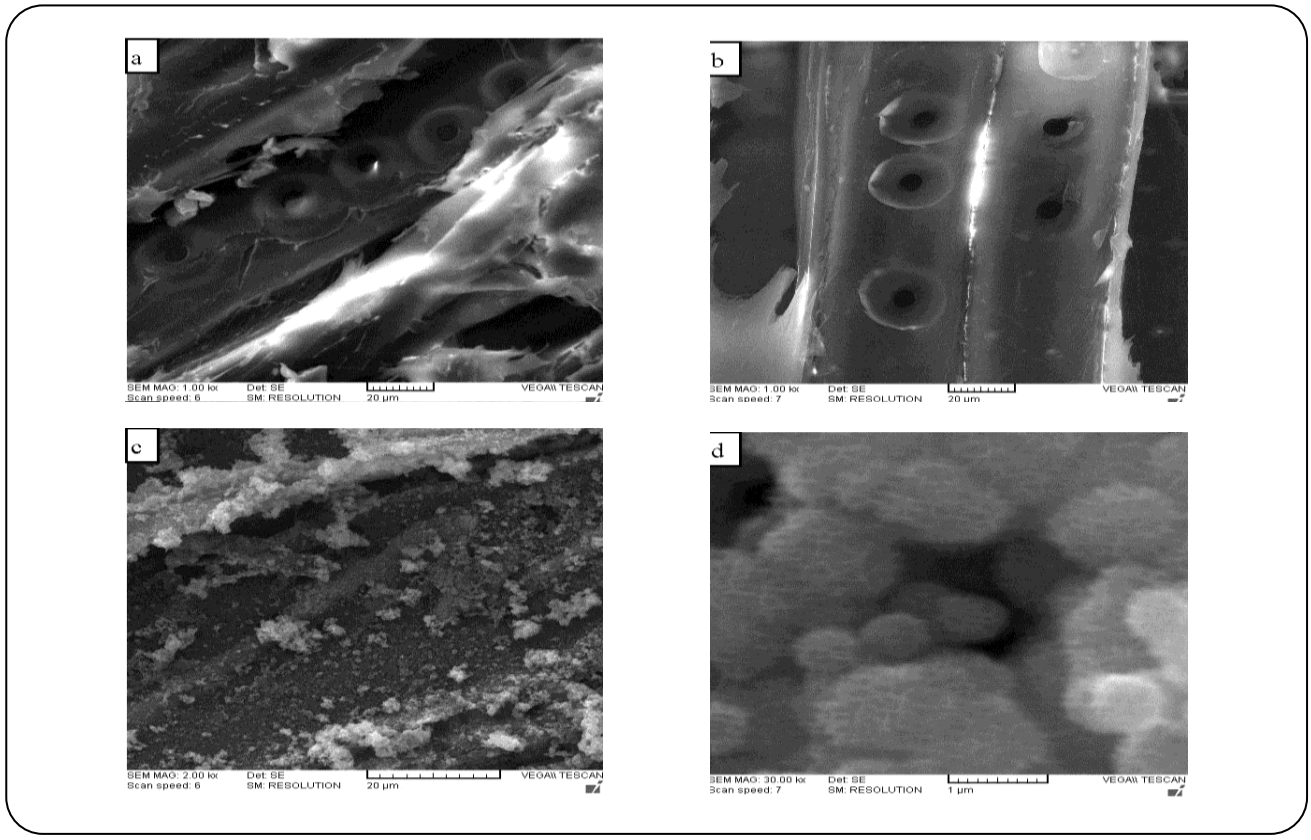

Fig. 3: SEM images of (a) untreated wood (b) WB (c, d) WB-NMO scaled to 20 and 1 micrometer, respectively.

has peeled back at some spots due to alkali treatment. The disappearance of the previous structural information in Fig. 3 (c) is due to the deposition of NMO on the surface of the wood particle (Tshabalala 2005). Fig. 3 (d) shows the high-magnification image of NMO particle, which is composed of uniform flower-like microsphere nanostructures with a diameter of 400-600 nm.

Effect of contact time and pH

As shown in Fig. 4 (a), the equilibrium time for Pb^{2+} adsorption on WB-NMO was determined in the batch experiment and found to be 240 min. The acidity of the solution is one of the most important factors affecting the sorption of metal ions. The effect of pH on the adsorption of Pb^{2+} was studied from 2.5 to 10, and results were shown in Fig. 4 (b).

Removal efficiencies (%) were very low at strong acidic medium and increased sharply at pH higher than 4. The removal efficiency has reached a plateau nearly pH value of 5. When solution pH increased from 2 to 5, the Pb^{2+} biosorption percentage increased from 16.0 to 94.8 %. Hence, the optimum pH of Pb^{2+} solution was determined as 5.0 and the rest of this study was carried out at this value.

Generally, at low pH values the surface of the adsorbent would be closely associated, by repulsive forces, with hydronium ions H_3O^+ to the surface functional groups, consequently decreasing the percentage adsorption of metal ions (*Madhava Rao et al.* 2006). As the solution pH increases, the onset of the metal hydrolysis and precipitation begins and therefore the onset of adsorption occurs before the beginning of hydrolysis. When the pH of the adsorbing medium was higher than the pH_{PZC} = 4.3, there was a corresponding increase in the de-protonation of the adsorbent surface, leading to a decrease in H^+ on the adsorbent surface. This creates more negative charges on the adsorbent surface, which favors the adsorption of positively charged species.

Effect of WB-NMO Dosage

The sorbent capacity for a given initial concentration of adsorbate was defined by sorbent dosage, which

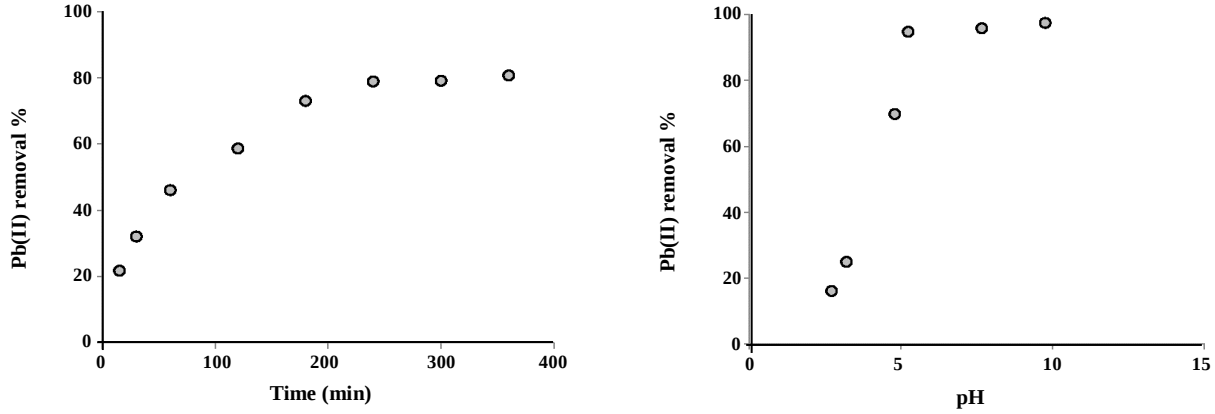

Fig. 4: a) Effect of agitation time on Pb^{2+} removal in batch experiment (v/m= 10 L/g), b) Effect of pH value on the Pb^{2+} adsorption onto WB-NMO (v/m= 200 L/g).

As a significant parameter, the effect of WB-NMO dosage on Pb^{2+} removal was studied by varying dosage for three initial concentrations (10, 25 and 60 mg/L). As clearly seen in Fig. 5, the sorption percentage of Pb^{2+} from solution was increased with the increase in WB-NMO content. This could be attributed to the availability of greater active sorption sites with increasing the WB-NMO content. With increasing WB-NMO content, the available sorption sites increase without any additional Pb^{2+} available in solution i.e. availability of fewer Pb^{2+} per unite mass of WB-NMO. This could explain the decrease in the equilibrium adsorption capacity q_e with increasing WB-NMO content (Fig. 5). The maximum removal of more than 97 % was observed at an adsorbent dosage of 0.5, 0.6 and 1.3 g/L for initial Pb^{2+} concentration of 10, 25 and 60 mg/L, respectively. Therefore, the choice of the adsorbent dose was made to be justified for economical purposes.

Effect of temperature

Temperature is an important factor in evaluating the mechanism and determining the sorption type. The effect of temperature on the Pb^{2+} adsorption mechanism on WB-NMO was studied with initial Pb^{2+} concentration of 30 mg/L, a pH of 5.0±0.2, m/v=0.02 to 1.0 g/L at three different temperatures of 295, 313 and 333 K.

Fig. 6 shows that the equilibrium sorption capacity of WB-NMO increases with temperature, indicating that a higher temperature favors Pb^{2+} removal by adsorption on WB-NMO. An increase in the amount of adsorption, with a rise in the temperature, may be due to higher adsorption caused by an increase in the thermal energy of the adsorbate. This indicates that the adsorption process is endothermic in nature. This effect is characteristic of a chemical reaction, or bond being involved in the sorption process with the increase in temperature, increasing the equilibrium conversion (*Turan et al.* 2007).

Adsorption kinetics

Adsorption kinetics is one of the most important aspects of the operation defining the efficiency of the process. In order to evaluate the kinetic mechanism that controls the adsorption process, the experimental data are interpreted by four kinetic models including the pseudo-first-order, the pseudo-second-order, intra-particle diffusion and Elovich models (*Salifu et al.* 2013).

The mathematical linear forms of pseudo first and second-order models are given in Eqs (3) and (4), respectively.

$$\ln(q_e - q_t) = \ln q_e - k_1 t \quad (3)$$

$$t/q_t = 1/k_2 q_e^2 + (1/q_e)t \quad (4)$$

Where q_e and q_t in (mg/g) are the adsorbed amounts of the adsorbate at equilibrium, and at any time respectively. k_1 (min^{-1}) and k_2 (g/mg min) are the first and second-order adsorption rate constants respectively, and *t* is the time in a minute. The adsorption rate constant k_2 can be used to calculate the initial adsorption rate h_0 as $h_0 = k_2 q_e^2$. The adsorption rate can be also predicted by the half-adsorption time $t_{1/2} = 1/k_2 q_e$, defined as the

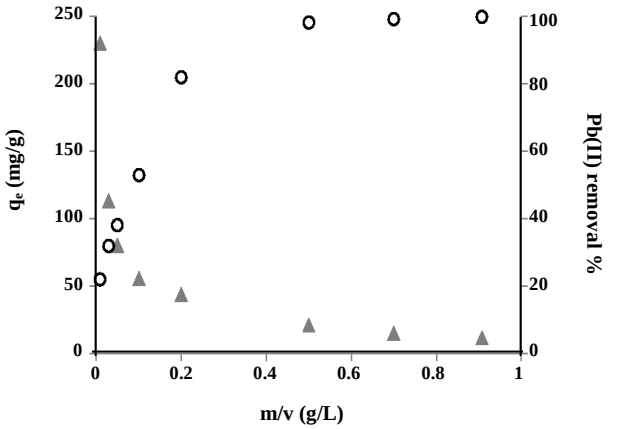

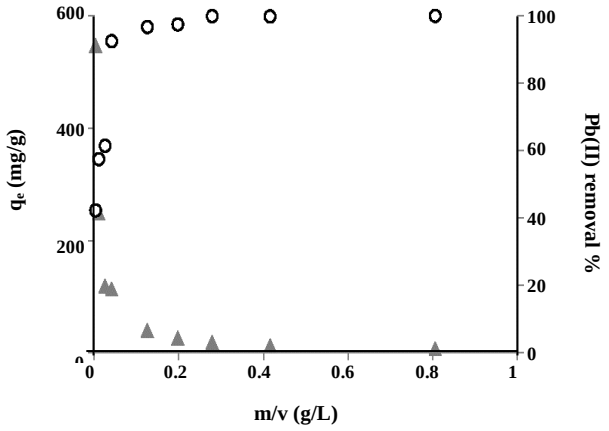

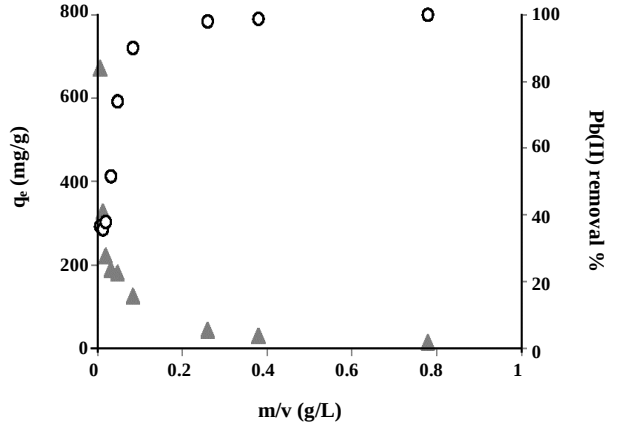

Fig. 5: Effect of the adsorbent amount on Pb^{2+} sorption by WB-NMO. c_0 (a) 10 mg/L, (b) 25 mg/L and (c) 60 mg/L, pH= 5.0±0.2, T= 295±2 K, time=240 min.

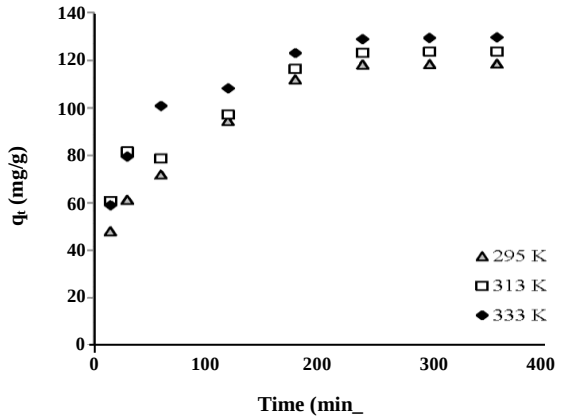

Fig. 6: Variation of adsorption capacity of Pb^{2+} on WB-NMO, with contact time at different temperature.

the time required for the adsorbent to take up half as much Pb^{2+} as its equilibrium value.

The Kinetic parameters and coefficients of determination for initial concentration (C_0= 25 mg/L) were calculated from the corresponding plot (Fig. 7) and listed in Table 1.

The values of coefficients of determination of pseudo-second-order kinetic model (0.997) are higher than those of the Elovich, pseudo first-order and intra-particle diffusion equations. Regarding Fig. 7 (b), straight lines were obtained in plotting t/q_t versus t and the results are presented in Table 1. It was noted that the best agreement of experimental data was with the pseudo-second-order kinetic model, with an adsorption capacity agreed with experimental results. Thus, it could be assumed that Pb^{2+} adsorption on WB-NMO follows second-order chemisorptions, with an initial sorption rate of 4.0 mg/g min, and a half-adsorption time $t_{1/2}$ of 31.6 min.

Elovich model, a useful kinetic model for describing chemisorption, was investigated based on Eq. (5), where a plot of the adsorbed Pb^{2+} q_t against $\ln t$ should yield a straight line. The constant α (mg/g min) is considered as the initial adsorption rate, and the β value is an indication of the number of sites available for adsorption.

$$q_t = 1/\beta \ln(\alpha\beta) + 1/\beta \ln t \quad (5)$$

As shown in Fig. 7 (c), it was found that the kinetics data for the WB-NMO/Pb^{2+} systems were well described by the Elovich model, which further supports the involvement of chemisorption in the adsorption mechanism.

Table 1: Kinetic parameters for adsorption of Pb^{2+} on WB-NMO composite.

$q_{e,exp}$ (mg g^{-1})	Pseudo-first-order			Pseudo-second-order				
	$k_1\times10^{-2}$	q_1	R^2	$k_2\times10^{-4}$	q_2	h_0	$t_{1/2}$	R^2
115	1.3	79.7	0.977	2.5	126.6	4.0	31.6	0.997
$q_{e,exp}$ (mg g^{-1})	Intra-particle diffusion			Elovich equation				
	k_t	C	R^2	α	β	R^2		
115	4.50	39.92	0.939	13.2	0.045	0.987		

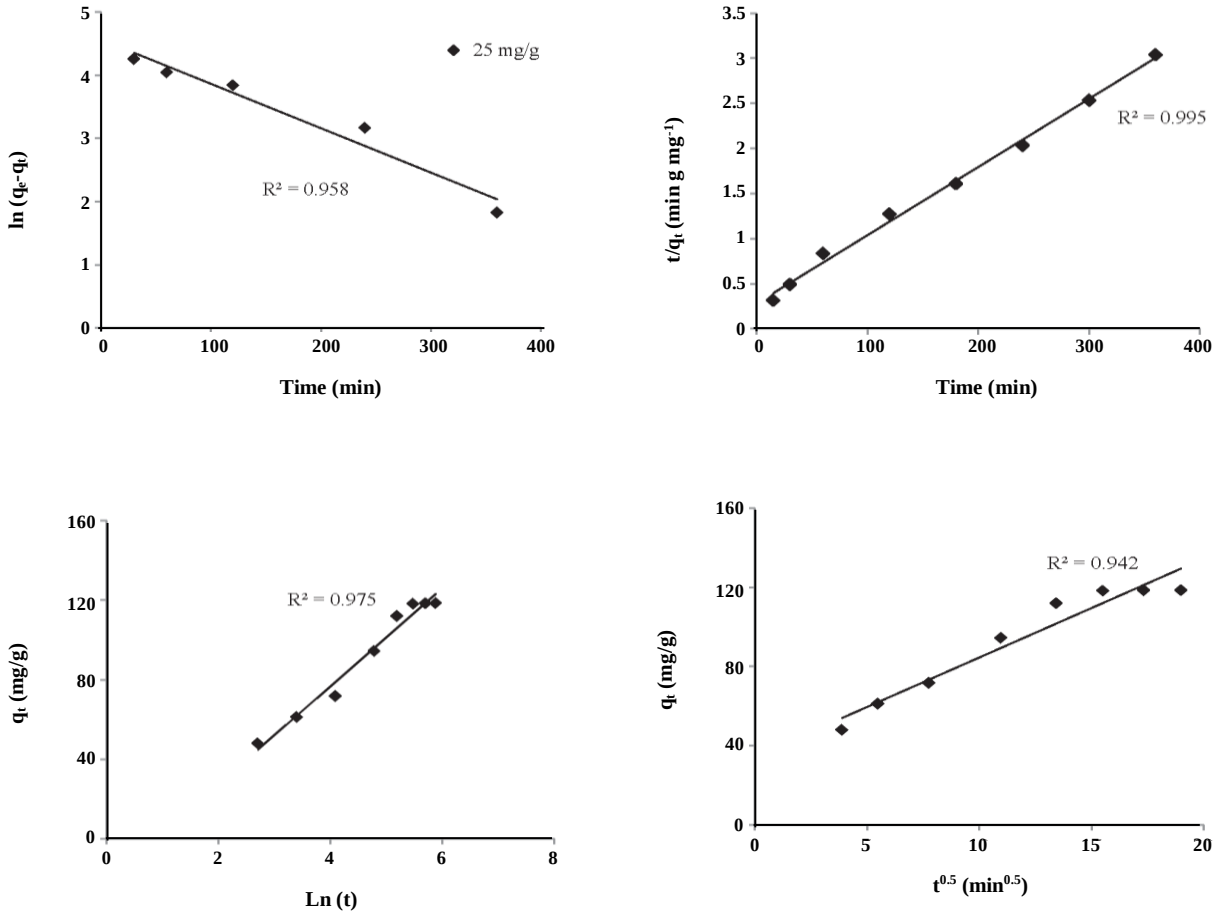

Fig. 7: The linear fitting of (a) Pseudo-first order, (b) Pseudo-second order, (c) Elovich equation and (d) Intra-particle diffusion models.

For better understanding the mechanism of Pb^{2+} adsorption on WB-NMO, and rate controlling step, the intra-particle diffusion model was used for fitting the experimental data.

The intra-particle diffusion model is commonly applied to predict the rate controlling step. The rate constant of intra-particle diffusion k_{id} (mg/g $min^{1/2}$) at stage i was determined using the following equation:

$$q_t = k_{id} t^{1/2} + C_i \quad (6)$$

Where c_i (mg/g) is the intercept at stage i. The value of c_i is related to the thickness of the boundary layer. The larger c_i represents the greater effect of the boundary layer on ion diffusion.

If intra-particle diffusion is involved in the adsorption process, a plot of q_t versus. $t_{1/2}$ should be linear. The rate-

limiting process is only due to intra-particle diffusion when the line passes through the origin. Otherwise, some other mechanism is also involved in the rate-controlling step alongside intra-particle diffusion.

Based on the R^2 value (Table 1), the intra-particle diffusion plays an important role in the adsorption of Pb^{2+} on WB-NMO. However, the linear plot did not pass through the origin (Fig. 7 (d). This indicates that the adsorption process is complex and both intra-particle diffusion and film diffusion (diffusion of Pb^{2+} across the boundary layer to the exterior surface of the adsorbent particles) contribute to the rate-determining step. As WB-NMO outer surface occupied with Pb^{2+}, the adsorption process in the later stages would be controlled by intra-particle diffusion through the pores for uptake at the interior surface of the adsorbent until equilibrium is reached. The boundary layer thickness (C) could give an insight about Pb^{2+} tendency to be adsorbed onto the adsorbent phase, where higher adsorption could be expected with higher C values. As shown in Table 1, C value (39.92) presents an important effect of the boundary layer on Pb^{2+} ion diffusion.

Adsorption isotherms

The equilibrium adsorption isotherm is fundamental in describing the interactive behavior between the adsorbate and adsorbent and is important in the design of adsorption systems.

To understand the interaction of Pb^{2+} with WB-NMO, it is important to establish the appropriate correlations for the equilibrium data. Three isotherm models; namely Langmuir, Freundlich, and Brunauer-Emmett-Teller (BET) were used to correlate the equilibrium data for Pb^{2+} removal. Linear regression is generally used to define the best fitted isotherm, and also the coefficients of determination are evaluated to compare the practicality of isotherm equation. The Langmuir isotherm is described by Eq. (7) (*Langmuir* 1918), and it supposes that adsorption takes place on a homogenous surface by monolayer sorption without interaction between adsorbed ions.

$$1/q_e = (1/k_L q_{max})(1/c_e) + 1/q_{max} \quad (7)$$

Where q_{max}(mg/g) and k_L(L/mg) are Langmuir constants which are related to maximum sorption capacity and energy of sorption, respectively. q_{max} and k_L can be calculated from the intercept and slope of the linear plot of $1/q_e$ versus $1/c_e$.

The empirical Freundlich isotherm explains monolayer sorption with a heterogeneous energetic distribution of active sites (*Salifu et al.* 2013). The linearized form is given in the following equation:

$$\ln q_e = \ln k_F + n \ln c_e \quad (8)$$

where k_F and n are the Freundlich constants that are related to the sorption capacity and intensity, respectively. They k_F can be calculated from the slope and intercept of the linear plot of lnq versus $\ln c_e$.

The Brunauer-Emmett-Teller (BET) is a theoretical equation considered as an extension of the Langmuir model for multilayer adsorption. The linear form of BET equation is given by:

$$c_e/(c_s - c_e)q_e = 1/k_B q_s + (k_B - 1/k_B q_s)(c_e/c_s) \quad (9)$$

where k_B is the equilibrium constant related to the interaction energy of adsorbate with the surface of the adsorbent, q_s(mg/g) is the maximum monolayer capacity and c_s(mg/L) is the adsorbate monolayer saturation concentration.

The initial concentration of Pb^{2+} could be an important factor affecting the adsorption process. This could be due to the driving forces provided by the initial concentration to overcome all mass transfer resistances of the metal ion between aqueous and solid phases. Thus, adsorption experiments were carried out using a different initial concentration of Pb^{2+} (10, 25 and 60 mg/L), with pH= 5.0±0.2 at a constant temperature of 295±2 K. Results were presented in Fig. 8 as a function of the equilibrium adsorption capacity, and the values obtained for the adsorption parameters of the three models studied were presented in Table 2.

Multilayer shapes of the adsorption isotherms were observed, consistent with a recent study on the adsorption of Cu, Cd, and Zn on Poplar wood sawdust (*Šćiban et al.* 2007). However, several studies concerning the adsorption of heavy metals onto wood have shown plots with a flattening at higher levels of metal concentration (*Kalavathy et al.* 2005; *Božić et al.* 2013; *H. U. Rahman et al.* 2005).

As can be seen from Table 2, the Langmuir and Freundlich coefficients of determination are relatively low, and the most precise match was acquired with

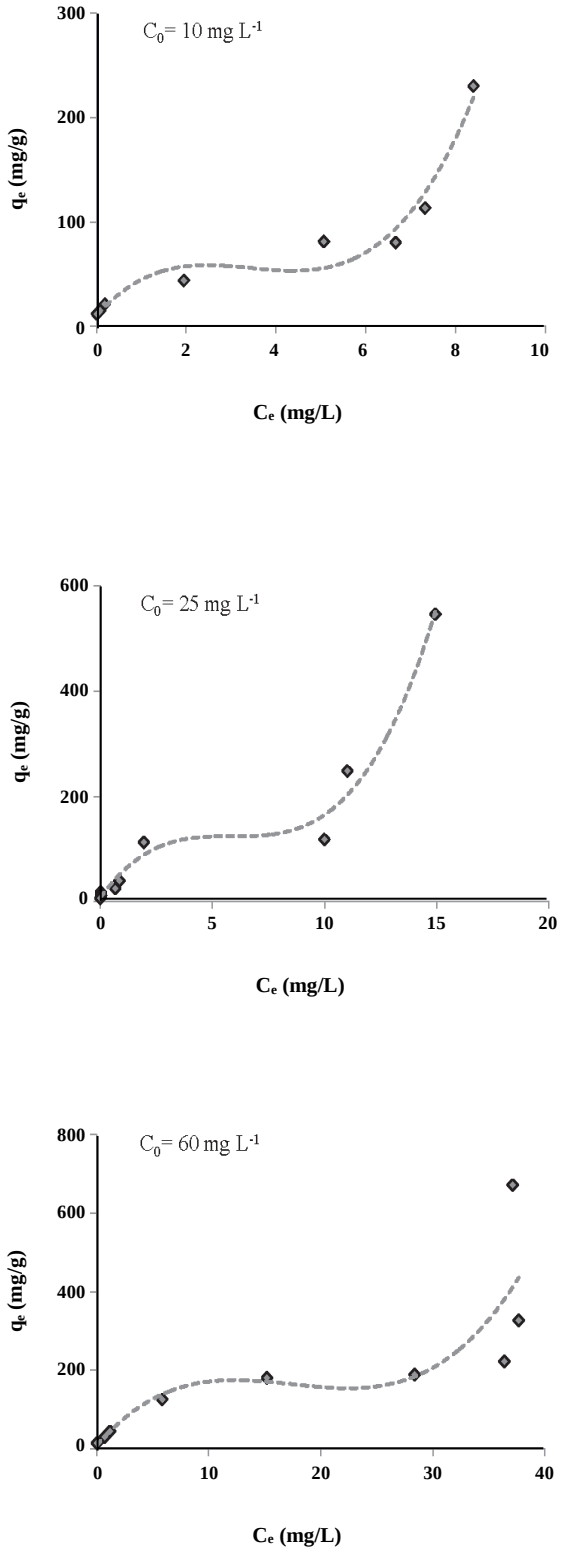

***Fig. 8*: Sorption isotherm of Pb^{2+} on WB-NMO. pH= 5.0±0.2, T= 295±2 K, time = 240 min.**

the BET model with R^2 = 0.979, 0.937 and 0.984 for c_0 = 10, 25 and 60 mg/L, respectively. In other words, the BET model confirmed that the adsorption of Pb^{2+} on WB-NMO is multilayer.

Comparing to other adsorbents in the literature, WB-NMO exhibited higher uptake properties of Pb^{2+} than many other adsorbents such as, kaolinite, Na-bentonite and modified magnetic adsorbents, reflecting of the potential application of WB-NMO on Pb^{2+} adsorption (*Yang et al.* 2010; *Sari et al.* 2007; *Zhu, Yehua et al.* 2012; *Jiang et al.* 2015; *Tran et al.* 2010; *Xu et al.* 2011).

Thermodynamic studies

Thermodynamic parameters, such as the Gibbs energy (ΔG^0), enthalpy (ΔH^0), and entropy (ΔS^0) are useful to evaluate the orientation and feasibility of the physicochemical adsorptive reaction, and provide information about the inherent energy and structural changes. They are determined by using the following equations (Eqs. (10), (11) and (12)):

$$k_d = \frac{q_e}{C_e} \tag{10}$$

$$\Delta G^o = -RT \ln k_D \tag{11}$$

$$\ln k_d = \frac{\Delta S^0}{R} - \frac{\Delta H^0}{RT} \tag{12}$$

Where R (8.3145 J/mol K) is the ideal gas constant, T (K) is the absolute temperature and k_D is the equilibrium constant for Pb^{2+} ion adsorption on WB-NMO. The values of changes of enthalpy ΔH^0 and entropy ΔS^0 are calculated from the slopes and intercepts of the plot of $\ln k_d$ vs. 1/T by using Eq. (10).

The enthalpy of the adsorption, ΔH^0, is a measure of the energy barrier that must be overcome by reacting molecules. The positive values of ΔH^0 indicate the endothermic behavior of the adsorption reaction and suggest that a large amount of heat is consumed to transfer Pb ions from aqueous into the solid phase. As suggested by *Nunes* and *Airoldi* (1999), the transition metal ions must give up a larger share of their hydration water before they can enter the smaller cavities. Such a release of water from the divalent cations will result in positive values of ΔS^0 (*Eren et al.* 2009).

The value of ΔS^0 can be used to identify whether the adsorption reaction is attributed to associative

Table 2: Langmuir, Freundlich and BET isotherm constants for Pb^{2+} adsorption on WB-NMO composite.

c_0 (mg/L)	Langmuir model			Freundlich model			BET model		
	k_L (L/mg)	q_{max} (mg/g)	R^2	k_F (L/g)	n	R^2	k_B	q_s (mg/g)	R^2
10	27.5	46	0.623	48.85	0.392	0.881	80	63	0.979
25	6.91	69	0.908	61.47	0.530	0.893	200	125	0.937
60	5.11	103	0.799	52.91	0.474	0.895	118	213	0.984

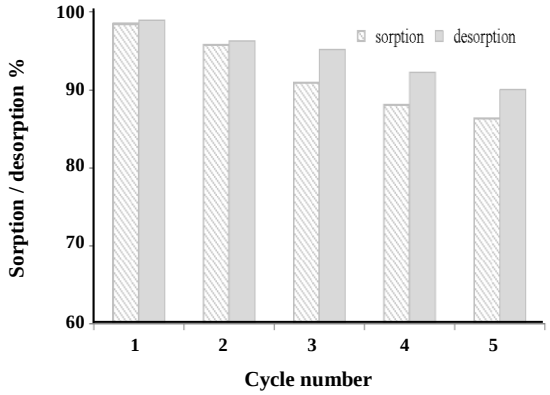

Fig. 9: Five cycles of Pb^{2+} sorption/desorption with HCl solution (0.2 mol/L) as the desorption agent. pH=5.0±0.2, T=295±2 K, time = 240 min, m/v = 1.5 g/L and c_0 =25 mg/L.

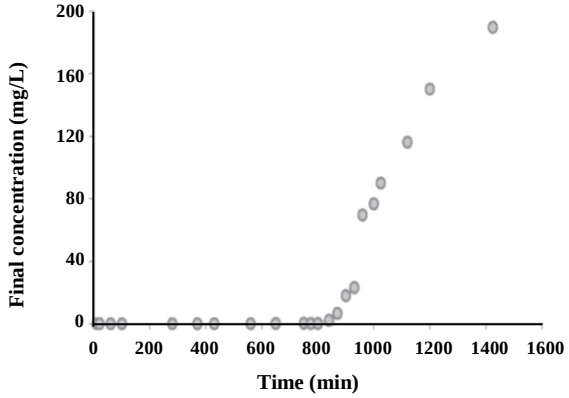

Fig. 10: Final concentration of Pb^{2+} in the effluent vs. contact time for wastewater.

or dissociative mechanism. Generally, entropy change $\Delta S^0 > -10$ J/mol K implies dissociative mechanism. The entropy changes in this work are positive, implying that the dissociative mechanism is involved in the adsorption processes.

The Gibbs energy change ranged from -9.4 kJ/mol at 295 K to -14.9 kJ/mol at 333 K. These negative values show that the adsorption process is feasible and spontaneous thermodynamically. Furthermore, the increase in ΔG^o with increasing temperature indicates that the adsorption is favorable at a higher temperature.

It was concluded that the temperature affects the adsorption process of metal ions onto WB-NMO, and a higher temperature provided more energy to enhance the adsorption rate.

Regeneration of WB-NMO composite

To enhance the economic value of the sorption process, desorption is considered as an important process in sorption studies, which helps to regenerate the spent adsorbent. As demonstrated in Fig. 4 (b), Pb^{2+} adsorption in acidic medium was relatively low, thus Pb^{2+} could be desorbed from spent adsorbent using acidic solution.

Results showed a low desorption percentage using HNO_3 solutions (> 40 %). The Pb^{2+} desorption efficiencies using HCl solutions were 70.5±1.6, 77.3±1.4, 82.3±0.9, 98.9±1.1, 99.2±1.3 and 99.1±1.2 % for HCl concentrations of 0.01, 0.05, 0.1, 0.5, 1.0 and 2.0 mol/L, respectively. As a result, the 0.5 mol L^{-1} HCl solution was chosen as a Pb^{2+} desorption solution.

The reusability of WB-NMO composite was studied in five sorption/desorption cycles using 0.5 mol/L HCl as a desorption agent. As shown in Fig. 9, the sorption percentage decreased from 98.5 % to 86.3% after five cycles. The recovery of Pb^{2+} from spent adsorbent decreased from 98.9% to 90.0%. Therefore, HCl solution can regenerate the adsorbent successfully, and the biosorbent composite material can be efficiently reused with lower production of residues.

Application of the composite to wastewater

The results of the column adsorption experiment, using a sample of industrial wastewater (initial Pb^{2+} ions concentration=20.0 mg/L), is presented in Fig. 10. As shown, a maximum concentration about 0.1µg/L of Pb^{2+} was present in solution during the first 9 h of the

operation of the column, after which the concentration was increased progressively, and reached the initial concentration after 24 h of operation.

The total Ca^{2+} concentration in the effluent was moderately decreased from 60±2 to 50±2 mg/L. The slight increase in the total concentration of Ca^{2+} confirmed the low effect of Ca^{2+} ions on the Pb^{2+} ions adsorption onto the WB-NMO. The test results confirmed that the prepared WB-NMO was a promising candidate for wastewater treatment.

CONCLUSIONS

The chemical modification with NaOH increased the reactivity of wood and allowed potassium permanganate to react with wood components resulting in the formation of active sites on which NMO precipitated and the composite WB-NMO produced. To evaluate the efficiency of the composite as a sorbent, the maximum uptake data of Pb^{2+} ions at room temperature was fitted to different kinetics and isotherms models. The Brunauer-Emmett-Teller (BET) model better described the system equilibrium and confirmed that the adsorption of Pb^{2+} from wastewater is a multilayer. The pseudo-second-order model best represented the experimental kinetics data with high initial adsorption rate, which confirmed that the chemical sorption could control the sorption process. Not only the intra-particle diffusion plays an important role in the adsorption of Pb^{2+} ions onto WB-NMO but there was also evidence that film diffusion contributes to the rate-determining step. Thermodynamic parameters demonstrated the endothermic nature of sorption, which could be explained by the partial dehydration of Pb^{2+} before its adsorption on the composite samples. WB-NMO could be efficiently reused, and HCl solution could regenerate the composite material successfully. In general, the WB-NMO is potentially a new alternative for Pb^{2+} removal from contaminated effluents allowing its subsequent reuse and application in industrial wastewater treatment. This study could encourage other researchers to use wood-metal oxide as an effective filtration amendment in treatment devices as well as to minimize the landfill space for wood waste.

Acknowledgements

It is a pleasure to acknowledge the support of Prof. I. Othman; the Director General of the Atomic Energy Commission of Syria, Prof. M. S. Al Masri; the head of protection and safety department and prof. Z. Ajji the head of the chemistry department.

Received : Nov. 1, 2016 ; Accepted : Nov. 20, 2017

REFERENCES

[1] WHO. "Guidelines for Drinking-Water Quality", (2008).

[2] Cechinel M.A.P., Souza S.M.A.G.U.d., Souza A.A.U.d., Study of Lead (II) Adsorption Onto Activated Carbon Originating From Cow Bone, *J Clean Prod*, **65**: 342-349 (2014).

[3] Özcan A.S., Gök Ö., Özcan A., Adsorption of Lead(II) Ions onto 8-hydroxy Quinoline-Immobilized Bentonite, *J Hazard Mater*, **161**(1): 499-509 (2009).

[4] Eren E., Afsin B., Onal Y., Removal of Lead Ions by Acid Activated and Manganese Oxide-Coated Bentonite, *J Hazard Mater*, **161**(2–3): 677-685 (2009).

[5] Al Abdullah J., Michèl H., Funel G., Féraud G., Distribution and Baseline Values of Trace Elements in the Sediment of Var River Catchment, Southeast France, *Environ Monit Assess*, **186**(12): 8175-8189 (2014).

[6] Li K., Zheng Z., Li Y., Characterization and Lead Adsorption Properties of Activated Carbons Prepared from Cotton Stalk by One-Step H_3PO_4 Activation, *J. Hazard Mater*, **181**(1-3): 440-447 (2010).

[7] Šćiban M., Radetić B., Kevrešan Ž., Klašnja M., Adsorption of Heavy Metals from Electroplating Wastewater by Wood Sawdust, *Bioresour Technol*, **98**(2): 402-409 (2007).

[8] Maliyekkal S.M., Lisha K.P., Pradeep T., A Novel Cellulose–Manganese Oxide Hybrid Material by In Situ Soft Chemical Synthesis and its Application for the Removal of Pb(II) from Water, *J. Hazard. Mater.*, **181**(1–3): 986-995 (2010).

[9] Eberhardt T.L., Min S.-H., Biosorbents Prepared from Wood Particles Treated with Anionic Polymer and Iron Salt: Effect of Particle Size on Phosphate Adsorption, *Bioresour. Technol.*, **99**(3): 626-630 (2008).

[10] Shi Z., Zou P., Guo M., Yao S., Adsorption Equilibrium and Kinetics of Lead Ion Onto Synthetic Ferrihydrites, *Iran. J. Chem. Chem. Eng. (IJCCE)*, **34**(3): 25-32 (2015).

[11] Sanchooli Moghaddam M., Rahdar S., Taghavi M., Cadmium Removal from Aqueous Solutions Using Saxaul Tree Ash, *Iran. J. Chem. Chem. Eng. (IJCCE)*, **35**(3): 45-52 (2016).

[12] Yousefpou, M., Modelling of Adsorption of Zinc and Silver Ions on Analcime and Modified Analcime Zeolites Using Central Composite Design, *Iran. J. Chem. Chem. Eng. (IJCCE)*, **36**(4): 81-90 (2017).

[13] Tajiki A., Abdouss M., Synthesis and Characterization of Graphene Oxide Nano-Sheets for Effective Removal of Copper Phthalocyanine from Aqueous Media, *Iran. J. Chem. Chem. Eng. (IJCCE)*, **36**(4): 1-9 (2017).

[14] Mohan D., Kumar H., Sarswat A., Alexandre-Franco M., Pittman Jr C.U., Cadmium and Lead Remediation Using Magnetic Oak Wood and Oak Bark Fast Pyrolysis Bio-Chars, *Chem. Eng. J.*, **236**: 513-528 (2014).

[15] Miró C., Baeza A., Salas A., Pastor-Valle J.f., Pastor-Villegas J., Adsorption of ^{241}Am And ^{226}Ra from Natural Water by Wood Charcoal, *Appl. Radiat. Isot.*, **66**(1): 95-102 (2008).

[16] Kalavathy M.H., Karthikeyan T., Rajgopal S., Miranda L.R., Kinetic and Isotherm Studies of Cu(II) Adsorption Onto H_3PO_4-Activated Rubber Wood Sawdust, *J. Colloid. Interface. Sci.*, **292**(2): 354-362 (2005).

[17] Wu F.-C., Tseng R.-L., Juang R.-S., Preparation of Highly Microporous Carbons From Fir Wood by KOH Activation for Adsorption of Dyes and Phenols from Water, *Sep. Purif. Technol.*, **47**(1–2): 10-19 (2005).

[18] Božić D., Gorgievski M., Stanković V., Štrbac N., Šerbula S., Petrović N., Adsorption of Heavy Metal Ions by Beech Sawdust – Kinetics, Mechanism and Equilibrium of the Process, *Ecol. Eng.*, **58**: 202-206 (2013).

[19] Hegazi H.A., Removal of Heavy Metals from Wastewater using Agricultural and Industrial Wastes as Adsorbents, *HBRC J.*, **9**(3): 276-282 (2013).

[20] Zhu Z., Zeng H., Zhu Y., Yang F., Zhu H., Qin H., Wei W., Kinetics and Thermodynamic Study of Phosphate Adsorption on the Porous Biomorph-Genetic Composite of A-Fe_2O_3/Fe_3O_4/C With Eucalyptus Wood Microstructure, *Sep. Purif. Technol.*, **117**: 124-130 (2013).

[21] Pehlivan E., Kahraman H., Sorption Equilibrium of Cr(VI) Ions on Oak Wood Charcoal (Carbo Ligni) and Charcoal Ash As Low-Cost Adsorbents, *Fuel Process Techno.l*, **92**(1): 65-70 (2011).

[22] Yargıç A.Ş., Yarbay Şahin R.Z., Özbay N., Önal E., Assessment of Toxic Copper(II) Biosorption from Aqueous Solution by Chemically-Treated Tomato Waste, *J. Clean. Prod.*, **88**: 152-159 (2015).

[23] Martín-Lara M.A., Blázquez G., Trujillo M.C., Pérez A., Calero M., New Treatment of Real Electroplating Wastewater Containing Heavy Metal Ions by Adsorption Onto Olive Stone, *J. Clean. Prod.*, **81**: 120-129 (2014).

[24] Semerjian, L., Equilibrium and Kinetics of Cadmium Adsorption from Aqueous Solutions using Untreated Pinus Halepensis Sawdust, *J. Hazard. Mater.*, **173**(1–3): 236-242 (2010).

[25] McLaughlan R.G., Hossain S.M.G., Al-Mashaqbeh, O.A., Zinc Sorption by Permanganate Treated Pine Chips, *J. Environ. Chem Eng*, **3**(3): 1539-1545 (2015).

[26] Ishaq M., Javed F., Amad I., Ullah H., Hadi F., Sultan S., Adsorption of Crystal Violet Dye from Aqueous Solutions Onto Low-Cost Untreated and NaOh Treated Almond Shell, *Iran. J. Chem. Chem. Eng. (IJCCE)*, **35**(2): 97-106 (2016).

[27] Chen H., He J., Facile Synthesis of Monodisperse Manganese Oxide Nanostructures and Their Application in Water Treatment, *J. Phys. Chem. C.*, **112**(45): 17540-17545 (2008).

[28] Al Lafi A.G., Al Abdullah J., Cesium and Cobalt Adsorption on Synthetic Nano Manganese Oxide: A Two Dimensional Infra-Red Correlation Spectroscopic Investigation, *J Mol Struct*, **1093**: 13-23 (2015).

[29] Al Abdullah J., Al Lafi A.G., Al Masri W.a., Amin Y., Alnama T., Adsorption of Cesium, Cobalt, and Lead Onto a Synthetic Nano Manganese Oxide: Behavior and Mechanism, *Water, Air, Soil Pollut*, **227**(7): 241 (2016).

[30] Al Lafi A.G., Al Abdullah J., Alnama T., Amin Y., Removal of Lead from Aqueous Solutions by Polyethylene Waste/Nano-Manganese Dioxide Composite, *J. Polym. Environ.*, **25**(2): 391-401 (2016).

[31] Greil P., Biomorphous Ceramics from Lignocellulosics, *J. Eur Ceram. Soc.*, **21**(2): 105-118 (2001).

[32] Davranche M., Lacour S., Bordas F., Bollinger J.C., An Easy Determination of the Surface Chemical Properties of Simple and Natural Solids, *J. Chem. Educ.*, **80**: 76-78 (2003).

[33] Wiedenhoeft, A. C.,Miller, R. B., "Structure and function of wood in Roger M. Rowell edt. Handbook of Wood Chemistry and Wood Composite", CRC Press: (2005).

[34] Morán J.I., Alvarez V.A., Cyras V.P., Vázquez A., Extraction of Cellulose and Preparation of Nanocellulose from Sisal Fibers, *Cellul.*, **15**: 149-159 (2008).

[35] Sreenivasan S., Bhamaiyer P., Iyer K.R.K., Influence of Delignification and Alkali Treatment on the Fine Structure of Coir Fibres (Cocos Nucifera), *J. Mater. Sci.*, **31**: 721-726 (1996).

[36] Sun Y., Cheng J., Hydrolysis of Lignocellulosic Materials for Ethanol Production: A Review, *Bioresour Technol*, **83**(1): 1-11 (2002).

[37] Gassan J., Bledzki A.K., Alkali Treatment of Jute Fibers: Relationship Between Structure and Mechanical Properties, *J. Appl Polym. Sci.*, **71**: 623-629 (1999).

[38] Jolly G., Dupont L., Aplincourt M., Lambert J., Improved Cu and Zn Sorption on Oxidized Wheat Lignocellulose, *Environ. Chem. Lett.*, **4**: 219-223 (2006).

[39] Tshabalala M.A., Surface Characterization in Roger M. Rowell edt. "Handbook of Wood Chemistry and Wood Composite", CRC Press (2005).

[40] Madhava Rao M., Ramesh A., Purna Chandra Rao G., Seshaiah K., Removal of Copper and Cadmium from the Aqueous Solutions by Activated Carbon Derived from Ceiba Pentandra Hulls, *J. Hazard. Mater.*, **129**(1–3): 123-129 (2006).

[41] Turan P., Doğan M., Alkan M., Uptake of Trivalent Chromium Ions from Aqueous Solutions Using Kaolinite, *J. Hazard. Mater.*, **148**(1–2): 56-63 (2007).

[42] Salifu A., Petrusevski B., Ghebremichael K., Modestus L., Buamah R., Aubry C., Amy G.L., Aluminum (hydr)oxide Coated Pumice for Fluoride Removal from Drinking Water: Synthesis, Equilibrium, *Kinetics and Mechanism*, *I*, **228**: 63-74 (2013).

[43] Langmuir I., The Adsorption of Gases on Plane Surfaces of Glass, Mica and Platinum, *J. Am. Chem. Soc.*, **40**(9): 1361-1403 (1918).

[44] Rahman H.U., Shakirullah M., Ahmad I., Shah S., Shah A.A., Removal of Copper (II) Ions from Aqueous Medium by Sawdust of Wood, *J. Chem. Soc. Pak.*, **27**(3): 233-238 (2005).

[45] Yang S., Zhao D., Zhang H., Lu S., Chen L., Yu X., Impact of Environmental Conditions on the Sorption Behavior of Pb(II) in Na-Bentonite Suspensions, *J. Hazard. Mater.*, **183**(1–3): 632-640 (2010).

[46] Sari A., Tuzen M., Citak D., Soylak M., Equilibrium, Kinetic and Thermodynamic Studies of Adsorption of Pb(II) from Aqueous Solution onto Turkish Kaolinite Clay, *J. Hazard. Mater.*, **149**(2): 283-291 (2007).

[47] Zhu Y., Hu J., Wang J., Competitive Adsorption of Pb(II), Cu(II) and Zn(II) onto Xanthate-Modified Magnetic Chitosan, *J. Hazard. Mater.*, **221–222**: 155-161 (2012).

[48] Jiang R., Tian J., Zheng H., Qi J., Sun S., Li X., A Novel Magnetic Adsorbent Based on Waste Litchi Peels for Removing Pb(II) from Aqueous Solution, *J. Environ. Manage.*, **155**: 24-30 (2015).

[49] Tran H.V., Tran L.D., Nguyen T.N., Preparation of Chitosan/Magnetite Composite Beads and Their Application for Removal of Pb(II) and Ni(II) from Aqueous Solution, *Mat. Sci. Eng. C.*, **30**(2): 304-310 (2010).

[50] Xu M., Zhang Y., Zhang Z., Shen Y., Zhao M., Pan G., Study on the Adsorption of Ca^{2+}, Cd^{2+} and Pb^{2+} by Magnetic Fe_3O_4 Yeast Treated with EDTA Dianhydride, *Chem. Eng. J.*, **168**(2): 737-745 (2011).

[51] Nunes L.M., Airoldi C., Some Features of Crystalline Titanium Hydrogenphos-Phate,Modified Sodium and n-Butylammonium Forms and Thermodynamics of Ionic Exchange with K^+ and Ca^{2+}, *Thermochim. Acta.*, **328**: 297-305 (1999).